Study of nanocrystalline VO_2 thin films prepared by magnetron sputtering and post-oxidation*

Luo Zhen-Fei(罗振飞)†, Wu Zhi-Ming(吴志明)‡, Xu Xiang-Dong(许向东), Wang Tao(王 涛), and Jiang Ya-Dong(蒋亚东)

School of Optoelectronic Information, State Key Laboratory of Electronic Thin Films and Integrated Devices, University of Electronic Science and Technology of China, Chengdu 610054, *China*

(Received 9 December 2009; revised manuscript received 12 April 2010)

Nanocrystalline VO_2 thin films were deposited onto glass slides by direct current magnetron sputtering and post-oxidation. These films undergo semiconductor–metal transition at 70 °C, accompanied by a resistance drop of two magnitude orders. The crystal structures and surface morphologies of the VO_2 films were characterized by x-ray diffraction (XRD) and atomic force microscope (AFM), respectively. Results reveal that the average grain size of VO_2 nanograins measured by XRD is smaller than those measured by AFM. In addition, Raman characterization indicates that stoichiometric VO_2 and oxygen-rich VO_2 phases coexist in the films, which is supported by x-ray photoelectron spectroscopy (XPS) results. Finally, the optical properties of the VO_2 films in UV-visible range were also evaluated. The optical band gap corresponding to 2p–3d inter-band transition was deduced according to the transmission and reflection spectra. And the deduced value, $E_{\mathrm{opt2p-3d}} = 1.81$ eV, is in good agreement with that previously obtained by theoretical calculation.

Keywords: nanocrystal, vanadium dioxide, magnetron sputtering, post-oxidation

PACC: 6140M, 8110

1. Introduction

Vanadium dioxide (VO_2, the space group is $P2_1/c$ below 68 °C[1]) exhibits a reversible semiconductor-metal transition (SMT) at 68 °C, accompanied by an abrupt change in optical, magnetic and electrical properties. Owing to the unique physical properties, VO_2 has been extensively studied experimentally and theoretically over the past decades since 1959.[2] From a practical perspective, vanadium dioxide shows great potential in a wide variety of applications, such as smart windows,[3] memory devices,[4] infrared detectors,[5] field effect transistor,[6] etc.

As is well known, some physical properties of crystals become greatly different from those of the bulk when the dimensions are in nanometer scale. So does vanadium dioxide. In the past decade, nanostructured VO_2 films have drawn a great deal of attention, because they exhibited distinct noticeable physical properties. Gentle *et al.*[7] deposited nanograin VO_2 thin films onto optically polished super-white glass by direct current (DC) magnetron sputtering at 450 °C. They found that thin films of nanograin vanadium dioxide in the metallic phase can combine very strong plasmonic response and a complete optical switch to the metal phase at transition temperature, with an incomplete switch in DC response. These cannot be found in large crystals or large grain size films. Wang *et al.*[8] grew nanocrystalline VO_2 thin films on Si_3N_4 surface by reactive ion beam sputtering and annealing in argon atmosphere at 450 °C for 60 min, and they found that the nanostructure films exhibited a phase transition temperature at 34–48 °C, which is much lower than that of single crystal VO_2. Wang *et al.*[9] reported that a large-scale array of aligned VO_2 nanorods with a large optical band gap of 2.7 eV can be grown on silicon substrate. In applications, nanostructured VO_2 used in optical switching,[10] microbolometer,[11] and photocatalyst[9] showed high performance.

In this paper, we prepared nanocrystalline VO_2 thin films on glass slides and investigated the electrical and optical properties. However, the vanadium–oxygen system is very complex due to the multivalent vanadium ions,[12] V^+, V^{2+}, V^{3+}, V^{4+} and V^{5+}; thus

*Project partly supported by the National Natural Science Foundation of China (Grant No. 60736005).

†Corresponding author. E-mail: zhfluo@yahoo.com.cn

‡Corresponding author. E-mail: zmwu@uestc.edu.cn

© 2010 Chinese Physical Society and IOP Publishing Ltd

it is quite difficult to control the composition precisely in the depositing process. For VO_2 thin film preparation, especially, deposition parameters are controlled carefully using various depositing methods, such as magnetron reactive sputtering, pulsed laser deposition, reactive ion beam sputtering, reactive evaporation, etc. In the case of DC magnetron reactive sputtering, target poisoning may occur during the deposition,[13] resulting in sputtering rate sharply decreasing. We overcame these disadvantages by a two-step method. First, we prepared metallic vanadium thin films by a common DC magnetron sputtering, and then the films were post-oxidized *in-situ*, through which nanocrystalline VO_2 thin films were successfully produced.

2. Experimental details

Nanocrystalline VO_2 thin film was deposited by DC magnetron sputtering and post-oxidation. Glass slides (with dimensions of $22\times22\times1.1$ mm^3) were used as the substrates. These substrates were first rubbed with cotton in diluted detergent solution, and then were ultrasonically cleaned in ethanol and acetone for 15 min, respectively. After that, the substrates were rinsed by deionized water thoroughly. Finally, the cleaned substrates were dried by N_2 gas, and then loaded into the vacuum chamber. After the sputtering chamber was evacuated by a turbo-molecular pumping down to an initial pressure of 2×10^{-3} Pa, Ar (99.999%) was introduced into the vacuum chamber, and then a DC power of 81 W was used to generate the glow discharge, the surface of vanadium target (99.99 %) was cleaned by pre-sputtering in Ar atmosphere for 20 min. After that, vanadium layers without oxygen content were deposited on the substrates by sputtering from the cleaned V target in the ultra-pure Ar (O_2/Ar ratio = 0%) atmosphere. During the depositing process, the deposition temperature was controlled at 70 ℃ automatically by a PID (Proportional Integral Differential) temperature controller. After deposition, the samples were annealed in the deposition chamber at 300 ℃ in ultra-pure oxygen (99.9999%) of 1.6 Pa for 45 min. The microstructures and physical properties of thin films were studied by employing several techniques afterwards.

The colours of thin films visible on glass slide substrates are yellow green. The film thicknesses are about 270 nm, which were measured by cross-section scanning electron microscope (SEM, JSM-5900LV) images. The square resistance–temperature curves of the samples were measured by using four-point probe equipped with a heater. The x-ray diffraction (XRD, Philip X Pert MPD with copper x-ray source, ($\lambda = 1.5406$ Å, (1 Å = 0.1 nm)) was employed to characterize the crystal structures. The surface morphologies of the films were characterized by atomic force microscope (AFM, SPA400 SER). The information of surface composition was acquired by using x-ray photoelectron spectroscopy (XPS, XSAM800). The transmittance and reflectance spectra were measured using UV-visible spectrophotometer (Pharma Spec-1700, Shimadzu Corporation).

3. Results and discussion

Figure 1 shows the XRD pattern in θ–2θ configuration between 10° and 80° for investigating the structure of the thin film prepared by sputtering and *in-situ* post-annealing. As can be seen clearly, two XRD peaks appear at $2\theta = 27.90°$ and $2\theta = 57.69°$, respectively. These can be attributed to the (011) and (022) reflections of VO_2 monoclinic phase.[14] Furthermore, according to the peak width at $2\theta = 27.90°$, the value of average VO_2 grain size can be estimated by using Scherrer formula[15]

$$t = 0.9\lambda/(\beta\cos\theta_{\rm B}), \tag{1}$$

where t is the average crystallite size, $\lambda = 1.542$ Å—Cu-Kα radiation wavelength, β is the value of full width at half maximum (FWHM), $\theta_{\rm B}$ is the Bragg angle. Putting the value of FWHM (0.4401°) into Eq. (1), the average crystallite size of VO_2 is estimated to be about 18 nm. This indicates that the sizes of VO_2 grains are in nanometer scale.

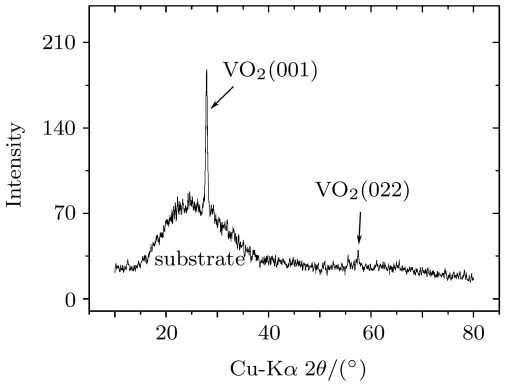


Fig. 1. XRD pattern of sample. The broad XRD peak in the region of 15–38 ℃ is due to the amorphous structure of glass substrate.

The surface morphologies of nanocrystalline VO_2 thin films are characterized by AFM, as presented in Fig. 2. It can be seen clearly that small particles grow vertically on the surface of substrate. The value of rms (square mean plane roughness) is 2.17 nm. This corresponds to rms-to-thickness ratio of 0.8%, indicating a smooth surface of the film. In addition, the sphere radius of particles in Fig. 2 is measured to be 35±10 nm, suggesting that fine particles of nanometer-scale can be grown by sputtering and post-oxidation. On the other hand, we notice that the particle size obtained by AFM measurement is larger than the average size of VO_2 nanograins estimated by XRD. This suggests that VO_2 nanograin is a portion of a particle, and the other portion contains vanadium oxides of other vanadium ions, such as V^{5+}, V^{3+}, etc.

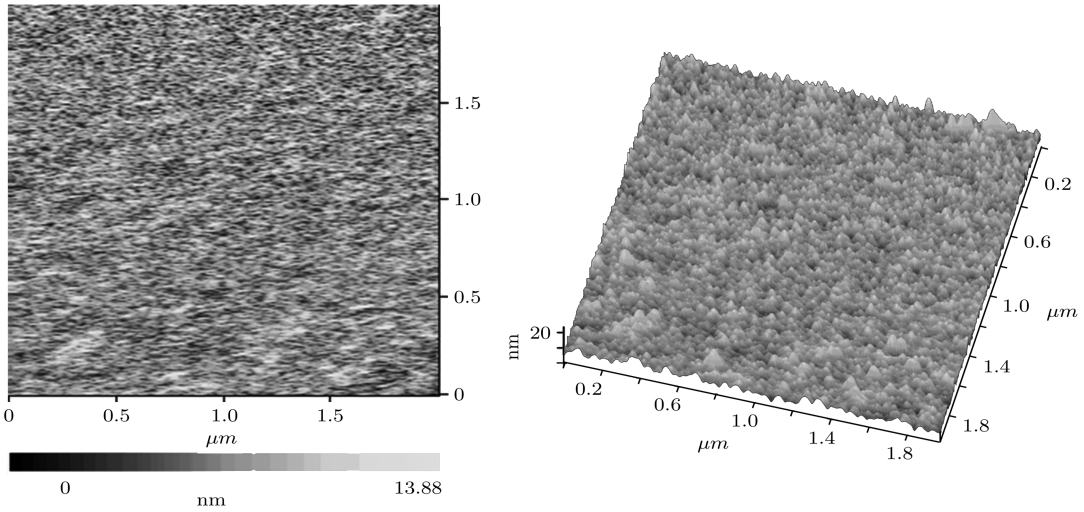


Fig. 2. Two-dimensional (left) and three-dimensional (right) AFM 2×2 μm^2 images of nanocrystalline VO_2 film.

The room-temperature Raman scattering (RS) spectra of samples is shown in Fig. 3. As can be seen, the peaks are broad and diffuse. This is attributed to the nanostructure of the film. The peak at 1000 cm^{-1} is associated with the $V^{5+} = O$ stretching mode related to the A_g symmetric vibrations of the shortest vanadium–oxygen bond.[16,17] The broad peak at about 225 cm^{-1} is assigned to the low frequency modes of VO_2. A fit of this broad peak is shown in the inset to clarify the position of separated peaks and the detailed data are recorded in Table 1. In comparison of the previous Raman studies of stoichiometric[18,19] and oxygen rich VO_2,[19,20] it is found that the low frequency modes of nanocrystalline VO_2 thin film in the present work can be divided into two groups. Group I contains modes of 221 cm^{-1}, 259 cm^{-1} corresponding to the stoichiometric VO_2 phase, and group II contains modes of 204 cm^{-1}, 240 cm^{-1}, 278 cm^{-1}, 306 cm^{-1} due to oxygen rich VO_2 phase. On the other hand, $V^{5+} = O$ mode can be observed in RS spectra, and this suggests that some of vanadium atoms were oxidized to V^{5+} after post-oxidation, supporting the RS modes of group II.

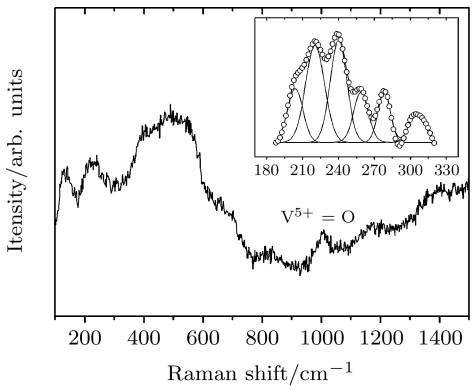


Fig. 3. Raman spectrum of nanocrystalline VO_2 film measured at room temperature. Inset: A fitted Raman spectrum in the range of 180 cm^{-1} to 330 cm^{-1}.

XPS is a powerful tool giving quantitative information about the chemical composition of sample surface. In this work, XPS analysis was applied to the investigation of the chemical composition of nanocrystalline VO_2 thin film. Figure 4 displays V 2p and O 1s

core level spectra of our samples, and the V $2p_{3/2}$ and V $2p_{1/2}$ peaks caused by the spin–orbit splitting have been fitted with mixed Lorentzian–Gaussian profiles after subtraction of a Shirley function using software XPSpeak4.1. Details of the fitted V 2p lines, such as binding energy (BE), area (background corrected area under the photoelectron emission lines) are given in Table 2. The results reveal that three kinds of vanadium ions exist in the film, and the concentration of V^{5+} ions is the highest. This indicates that, even after the post-annealing in the oxygen atmosphere, the vanadium atoms in the film surface layer were not all oxidized to the ions of highest valence state, namely V^{5+}. The distribution of ion-concentration can be explained on the basis of diffusion and oxidation as follows. When the oxygen atoms are adsorbed by the nanocrystalline VO_2 film, two types of atomic concentration gradients are formed. One originates from the oxygen atoms attempting to diffuse into the inner portion of the film, and the other is attributed to the metallic vanadium atoms trying to diffuse to the surface. As a result, V^{5+} ions on the surface are reduced due to the diffusing metallic vanadium atoms, and hence a mixture of vanadium ions of different valence states is formed.

Table 1. Comparison of the Raman data previously reported. All values are in unit cm^{-1}.

present work	single crystal VO_2[18]	stoichiometric single crystal VO_2[19]	oxygen rich single crystal VO_2[19]	oxygen rich VO_2 films[20]
204	199	191	202	201
221	225	223		
240			232	226
259	259	262	266	272
278	265			
306	313	310	305	295

Table 2. Binding energy (BE) and area of the fitted V 2p lines of the nanocrystalline VO_2 film.

	V^{5+} $2p_{3/2}$	V^{4+} $2p_{3/2}$	V^{3+} $2p_{3/2}$	V^{5+} $2p_{1/2}$	V^{4+} $2p_{1/2}$	V^{3+} $2p_{1/2}$
BE/eV	517.5	516.2	514.8	525.2	523.6	522.0
Area	2967.1	1930.9	932.9	1190.3	988.3	584.4

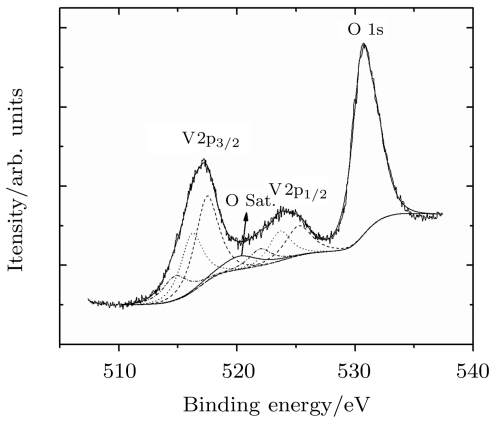


Fig. 4. XPS spectra of nanocrystalline VO_2 film.

In order to investigate the electrical property of nanocrystalline VO_2 thin films, we mounted the samples on a flat heater, and then placed four-point probe at the film surface, the temperature was measured from room temperature (RT = 26 °C) to 84 °C using a thermocouple with a measurement accuracy of 0.1 °C. Square resistance–temperature (R_{sq}–T) curve of the nanocrystalline VO_2 film is plotted in Fig. 5. It can be seen that, in the temperature range of 26 °C to 66 °C, R_{sq}–T curve shows good linearity, indicating a typical semiconducting phase, and then a resistance drop of two orders occurs when the film undergoes semiconductor–metal transition (SMT) at 70 °C. This SMT amplitude is about 2–3 orders lower than that of single crystal VO_2, due to the small VO_2 grains of nanometer scale. It is interesting to note that the transition temperature (T_{SMT} = 70 °C obtained from the derivative of R_{sq}–T curve) is slightly higher than the previously reported value, typical 67 °C. This can be attributed to the stress effect[21] associated with the lattice mismatch between the stoichiometric VO_2 and oxygen-rich VO_2 phases. Temperature coefficient of resistance (TCR) is an important parameter in applications, for instance, infrared detector and temper-

ature sensor. Based on the curve provided by Fig. 5, we can calculate TCR according to the relation.

$$TCR = \frac{1}{R_{\rm sq}} \frac{{\rm d}R_{\rm sq}}{{\rm d}T}. \quad (2)$$

We obtain the TCR at room temperature (RT = 26 °C) of the sample as: $TCR = -3.5\%/°C$. This TCR value is much higher than that of nanocrystalline VO_2 thin film prepared using sputtering and oxidation by Wang *et al.*[22]

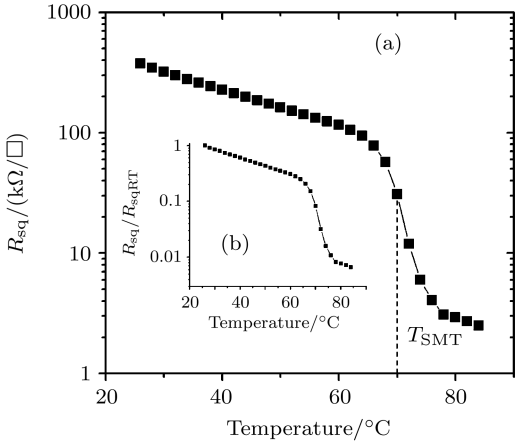


Fig. 5. Square resistance as a function of temperature of nanocrystalline VO_2 film. (a) $R_{\rm sq}$–T curve, (b) $R_{\rm sq}/R_{\rm sqRT}$ ratio versus temperature.

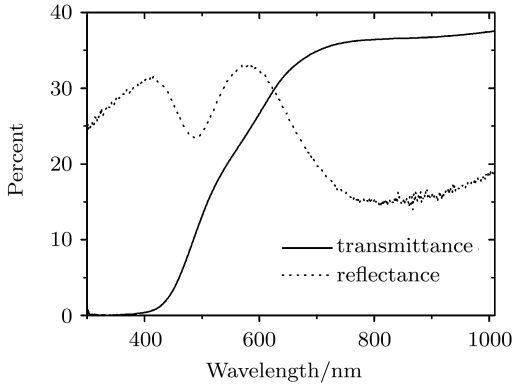


Fig. 6. Optical transmission and reflection spectra of nanocrystalline VO_2 films.

The room temperature UV-visible transmission and reflection spectra of nanocrystalline VO_2 thin films are shown in Fig. 6. As can be seen, the film exhibits low absorption in the wavelength region 650–1100 nm, and the transmittance decreases sharply for wavelengths below 600 nm. A shoulder can be observed at about 500 nm, in comparison with the hollow-shape transmission spectra measured by Lin *et al.*[23] According to the reflection spectra, it can be believed that this shoulder is attributed to the destructive interference of light reflected from the two interfaces in the air-nanocrystalline VO_2-glass system.

The optical band gap ($E_{\rm opt}$) corresponds to the minimum energy difference between the valence and conduction bands in electronic transition. According to the inter-band absorption theory, the optical band gap of film can be evaluated by the relations as follows:[24]

$$Tr = (1-R)^2 \exp(-\alpha d)/[1 - R^2 \exp(-2\alpha d)]$$
$$\approx (1-R)^2 \exp(-\alpha d), \quad (3)$$
$$(\alpha h\nu) = B(h\nu - E_{\rm opt})^n, \quad (4)$$

where Tr is the transmittance, R the reflectance, α the absorption coefficient, d the film thickness, $h\nu$ the incident photon energy, B the edge width parameter, n the exponent; and n can take the values of 2, 3, 1/2, 3/2 for different electronic transitions as indirect-allowed, indirect-forbidden, direct-allowed and direct-forbidden transitions, respectively. Figure 7 shows the plot of $(\alpha h\nu)^{1/2}$ versus $h\nu$ of the film. It is found that

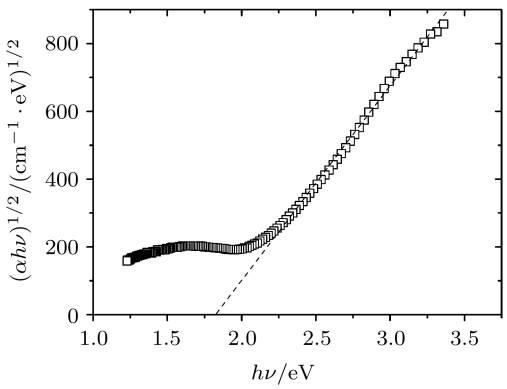


Fig. 7. Plot of $(\alpha h\nu)^{1/2}$ versus photon energy of nanocrystalline VO_2 films.

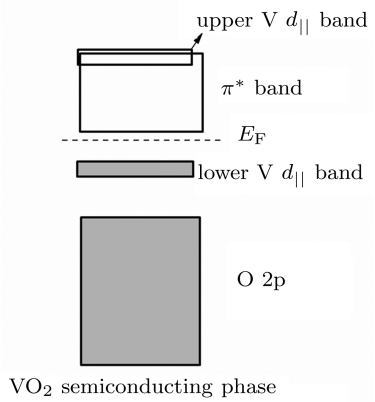


Fig. 8. Schematic energy band system of semiconducting VO_2.[25]

experimental data fit better when n is 2, suggesting the indirect-allowed transition. The electronic band structure of VO_2 contains a lower occupied O 2p band, and the upper band system is formed by anti-bonding V 3d orbital. The V 3d band system consists of an occupied V 3d band below the Fermi level and an unoccupied V 3d band above the Fermi level. A schematic energy band diagram of semiconducting VO_2 is shown in Fig. 8. Based on the band structure, the optical transitions in the wavelength of UV-visible region can be divided into two types: 2p–3d inter-band transition and 3d–3d intra-band transition.[25] According to Eq. (4), the value of optical band gap corresponding to 2p–3d inter-band transition is $E_{\mathrm{opt2p-3d}} = 1.81$ eV. This value is in good agreement with that theoretically calculated by Caruthers *et al.*[26] They reported that the top of the occupied O 2p band is located at 1.8 eV below the bottom of the unoccupied V 3d band.

4. Conclusions

In this paper, we have shown that nanocrystalline VO_2 thin films could be prepared by DC magnetron sputtering and post-oxidation. The R_{sq}–T curve of the films shows typical semiconducting property below 66 °C and exhibits a resistance drop of two orders when the film undergoes semiconductor–metal transition at 70 °C. The TCR value in the semiconducting phase is $TCR = -3.5\%/°\mathrm{C}$. Raman and XPS results reveal that the nanocrystalline VO_2 films consist of stoichiometric VO_2 and oxygen-rich VO_2 phases. The results of optical measurement indicate that 2p–3d inter-band transition occurs as the incident UV-visible photons are absorbed by the film. The value of optical band gap deduced from transmission and reflection spectra is $E_{\mathrm{opt2p-3d}} = 1.81$ eV, which is in good agreement with the previously theoretical calculation.

References

[1] Leroux C, Nihoul G and Tendeloo G Van 1998 *Phys. Rev.* B **57** 5111

[2] Morin F J 1959 *Phys. Rev. Lett.* **3** 34

[3] Babulanam S M, Eriksson T S, Niklasson G A and Granqvist C G 1987 *Solar Energy Mater.* **16** 347

[4] Balberb S and Trokman J 1977 *Appl. Phys.* **46** 2111

[5] Wang H C, Yi X J, Huang G, Xiao J, Li X W and Chen S H 2004 *Infrared Physics and Technology* **45** 53

[6] Kim H T, Chae B G, Youn D H, Maeng S L, Kim G, Kang K Y and Lim Y S 2004 *New J. Phys.* **6** 52

[7] Gentle A, Maaroof A I and Smith G B 2007 *Nanotechnology* **18** 025202-1

[8] Wang H C, Yi X J, Lai J J and Li Y 2005 *Chin. Phys. Lett.* **22** 1746

[9] Wang Y Q, Zhang Z J, Zhu Y, Li Z C, Vajtai R, Ci L J and Ajayan P M 2008 *ACS Nano* **2** 1492

[10] Wang H C, Yi X J and Li Y 2005 *Opt. Commun.* **256** 305

[11] He S W, Huang Y, Dai J, Lai J J, Wang X Z and Yi X J 2007 *Chin. J. Mater. Research* **21** 609 (in Chinese)

[12] Griffiths C H and Eastwood H K 1974 *J. Appl. Phys.* **45** 2201

[13] Theil J A, Kusano E and Rockett A 1997 *Thin Solid Films* **298** 122

[14] Manning T D and Parkin I P 2004 *Polyhedron* **23** 3087

[15] Ruzmetov D, Senanayake S D and Ramanathan S 2007 *Phys. Rev.* B **75** 195102

[16] Abello L, Husson E, Repelin Y and Lucazeau G 1983 *Spectrochimica Acta* A **39** 641

[17] Madhuri K V, Rao K S, Naidu B S, Hussain O M and Pinto R 2002 *J. Mater. Sci.* **13** 425

[18] Schilbe P 2002 *Physica* B **316–317** 600

[19] Parker J C 1990 *Phys. Rev.* B **42** 3164

[20] Wang X J, Liang C J, Guan K P, Li D H, Nie Y X, Zhu S O, Huang F, Zhang W W and Cheng Z W 2008 *Chin. Phys.* B **17** 3512

[21] Muraoka Y, Ueda Y and Hiroi Z 2002 *J. Phys. Chem. Solids* **63** 965

[22] Wang H C, Yi X J, Huang G, Xiao J and Chen S H 2003 *Semiconductor Optoelectronics* **24** 280 (in Chinese)

[23] Lin L B, Lu T C, L Q, Lu Y and Feng X D 2002 *Surface and Coating Technology* **158–159** 530

[24] El Mandouh Z S and Selim M S 2000 *Thin Solid Films* **371** 259

[25] Abe H, Terauchi M, Tanaka M, Shin S and Ueda Y 1997 *Jpn. J. Appl. Phys.* **36** 165

[26] Caruthers E and Kleinman L 1973 *Phys. Rev.* B **7** 3760